RESEARCH ARTICLE

Development of Epigallocatechin 3-gallate-Loaded Hydrogel Nanocomposites for Oral Submucous Fibrosis

Chetan Hasmukh Mehta[1] · Varalakshmi Velagacherla[1] · Suman Manandhar[2] · Yogendra Nayak[2] ·
Sreedhara Ranganath K Pai[2] · Shruthi Acharya[3] · Usha Yogendra Nayak[1]

Abstract

Oral submucous fibrosis (OSF) is a chronic progressive disease associated with increased collagen deposition and TGF-β1 release. The current therapy and management have been a limited success due to low efficacy and adverse drug reactions. This study aimed to evaluate epigallocatechin 3-gallate (EGCG) encapsulated nanoparticles loaded mucoadhesive hydrogel nanocomposite (HNC) for OSF. Developed HNC formulations were evaluated for their permeation behaviour using *in vitro* as well as *ex vivo* studies, followed by evaluation of efficacy and safety by *in vivo* studies using areca nut extract-induced OSF in rats. The disease condition in OSF-induced rats was assessed by mouth-opening and biochemical markers. The optimized polymeric nanoparticles exhibited the required particle size (162.93 ± 13.81 nm), positive zeta potential (22.50 ± 2.94 mV) with better mucoadhesive strength (0.40 ± 0.002 N), and faster permeation due to interactions of the positively charged surface with the negatively charged buccal mucosal membrane. HNC significantly improved disease conditions by reducing TGF-β1 and collagen concentration without showing toxicity and reverting the fibroid buccal mucosa to normal. Hence, the optimized formulation can be further tested to develop a clinically alternate therapeutic strategy for OSF.

Keywords *ex vivo* permeation and retention · epigallocatechin 3-gallate · *in vivo* efficacy and safety studies · mucoadhesive hydrogel nanocomposite · oral submucous fibrosis

Introduction

Oral submucous fibrosis (OSF) is one of the most dangerous and chronic progressive malignant oral diseases, which leads to oral cancer. Among various causative factors, chewing areca nut plays an important role in the progression of OSF [1, 2]. The arecoline, the major component in areca, penetrates through the oral mucosal epithelial membrane and interacts with connective tissue components, thus inducing the proliferation of fibroblasts and collagen concentration enhancement by disturbing collagen synthesis and degradation [1, 3]. The habit control, physiotherapy, drugs, laser treatment, nutritional and surgical intervention are options for treating OSF [4, 5]. However, these modalities will only relieve the symptoms and not complete remidy. The mainstay of drug treatment includes corticosteroid and betamethasone injections (BTM Inj.), which have several adverse effects such as edema, adrenal insufficiency, increased risk of infections, osteonecrosis, and myopathy [6].

The effects of polyphenols have been reported in the past for the treatment of OSF, and EGCG was found to be better complementary to the current therapy [7, 8]. *In silico* studies, it was proved that the EGCG acts on multiple targets. Compared to other polyphenols, EGCG was effective in *in vitro* safety studies and efficient in reducing the expression of collagen mRNA (type-1A2 and 3A1) and TGF-β1 [9]. EGCG hydrogel showed significant improvement in OSF condition by reducing collagen and TGF-β1 concentrations and improving mouth-opening in rat models of OSF [9]. However, EGCG has a very short half-life of 3-4 h and is

✉ Usha Yogendra Nayak
  usha.nayak@manipal.edu

1 Department of Pharmaceutics, Manipal College
   of Pharmaceutical Sciences, Manipal Academy of Higher
   Education, Manipal 576104, Karnataka, India

2 Department of Pharmacology, Manipal College
   of Pharmaceutical Sciences, Manipal Academy of Higher
   Education, Manipal 576104, Karnataka, India

3 Department of Oral Medicine and Radiology, Manipal
   College of Dental Sciences, Manipal, Manipal Academy
   of Higher Education, Manipal 576104, Karnataka, India

susceptible to oxidation in the presence of sunlight [10]. Hence, in our previous study, to improve the stability and to provide localised delivery, lipidic nanoparticles of EGCG-loaded mucoadhesive hydrogel named NanoCubogel were formulated, which showed better *ex vivo* permeation and its retention through the porcine buccal mucosal membrane [11]. Polymeric nanoparticles are more stable and easier to prepare as compared to lipidic nanoparticles. In addition to the above advantages, the controlled release behaviour of the drug can be maintained and convenient for surface modifications [12]. Therefore, polymeric nanoparticles loaded hydrogel can be preferred over the lipidic nanoparticles embedded hydrogel (NanoCubogel) [11].

Hydrogel nanocomposites (HNC) are hybrid materials composed of organic (polymeric nanoparticles, micelles, polymerosomes, dendrimers, and liposomes) and inorganic nanoparticles (inorganic clay nanoparticles, silica, silicates, hydroxyapatite, calcium phosphate, quantum dots) embedded into the hydrogels [13]. Incorporation of the drug into nanoparticles reduces the effect of burst release and enhances the steadiness or stability by providing sustained or controlled release. This formulation has various advantages over other formulations, such as longer retention, dosage flexibility increments, aesthetic appearance, and patient compliance improvement, as it is user-friendly [14]. The main aim of incorporating the EGCG into the nanoparticle is to hold the drug efficiently, avoid the burst release of drug, enhance drug stability, and transport it to the desired site at the required concentration with sustained or controlled release of the drug. The mucoadhesive hydrogel will withstand the physiological shear stress [15, 16]. In addition to this, a positive charge on the surface will help to permeate the buccal mucosal membrane faster [17].

Hence, in the current study, a mucoadhesive HNC formulation loaded with EGCG polymeric nanoparticles was prepared and evaluated for mucoadhesiveness, *in vitro* behaviour of EGCG release, *ex vivo* permeation, and *in vivo* efficacy on OSF rat model.

Materials and Methods

Materials

The (-)-Epigallocatechin 3-Gallate hydrate (EGCG) was purchased from TCI Chemicals, India. Poly(lactic-co-glycolic acid) (PLGA, 50:50) was procured from Yarrow Chem Products, Mumbai, India. Octadecylamine and polyvinyl alcohol (PVA, 87-89% hydrolyzed, mol. Wt. 13,000–23,000) were procured from Sigma Aldrich, India. Lubrizol, Mumbai, India, provided Carbopol-980 gelling agent. The procurement of areca nut extract was from Vital Herbs, Delhi, India. Collagen type-1-alpha-1 (COL1a1) and transforming growth factor-1 (TGF-β1) ELISA kits were procured from Elabscience and Maxome Labsciences, Bangalore, India, respectively. Betamethasone injection I.P. was procured from the Kasturba Hospital, Manipal, India.

Methods

Preparation and Evaluation of PLGA Nanoparticles and Hydrogel Nanocomposite

The schematic representation of EGCG-PLGA nanoparticle preparation followed by hydrogel nanocomposite (HNC) formulation is shown in Fig. 1. PLGA nanoparticles loaded with EGCG were prepared by modified double emulsion method in two steps such as the preparation of primary emulsion using high-speed homogenization (HSH, IKA T25 digital, Ultra-Turrax, Germany) followed by secondary emulsion using probe sonication (PS, Sonics Vibra-Cell, USA). Octadecylamine was used to modify the nanoparticle surface charge as per the published literature [18–20]. Several trials were taken by varying the material and instrument parameters for PLGA nanoparticle preparation and octadecylamine-modified nanoparticles encapsulated with EGCG are shown in Table I [21].

Fig. 1 EGCG-PLGA nanoparticle preparation and hydrogel nanocomposite (HNC) formulation. PVA: Polyvinyl alcohol; EGCG: Epigallocatechin 3-gallate; DCM: Dichloromethane
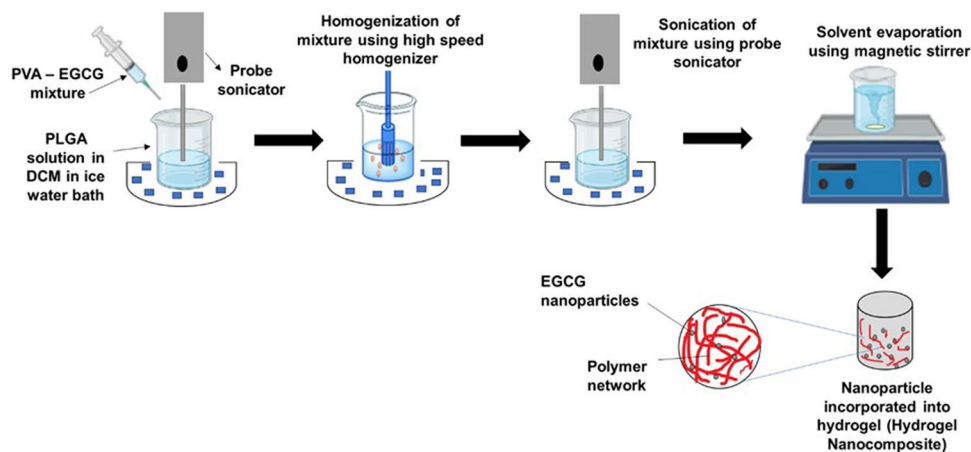
Table I Trials Taken for the Preparation of PLGA Nanoparticles

Trial No.	A (mg)	B (mg)	C (mg)	D (mL)	E (mL)	F (mL)	G (mL)	H (Time, Pulse, Amplitude)	I Speed (rpm)	I Time (Min.)	J Time (Min.)	J Pulse On/Off (sec.)	J Amplitude (%)	K (nm)	L	M (mV)
1	5	25	-	2	2	2	-	2, 10/2, 40	10000	5	No Sonication			677.47 ± 23.52	0.83 ± 0.10	-13.27 ± 0.25
2	5	25	-	2	2	0.5	-	2, 10/2, 40	10000	5	5	10/2	40	150.4 ± 3.37	0.1 ± 0.01	-22.2 ± 2.23
3	5	25	-	2	2	2	-	2, 10/2, 40	10000	5	5	10/2	40	177.5 ± 7.02	0.25 ± 0.03	-18.3 ± 0.35
4	5	50	-	2	2	0.5	-	2, 10/2, 40	10000	5	5	10/2	40	197.4 ± 13.29	0.21 ± 0.02	-21.3 ± 1.07
5	5	25	-	2	2	0.5	-	2, 10/2, 40	10000	10	5	10/2	40	207.0 ± 12.11	0.38 ± 0.05	-20.8 ± 0.51
6	5	25	-	2	2	0.5	-	2, 10/2, 40	15000	5	5	10/2	40	222.8 ± 14.55	0.31 ± 0.04	-20.3 ± 1.06
7	5	25	-	2	2	0.5	-	2, 10/2, 40	15000	10	5	10/2	40	336.9 ± 3.50	0.41 ± 0.06	-9.72 ± 1.01
8	5	25	-	2	1	0.5	-	2, 10/2, 40	10000	5	5	10/2	40	175.4 ± 2.60	0.14 ± 0.01	-21.6 ± 2.53
9	5	25	-	2	2	0.5	-	2, 5/2, 40	10000	5	5	10/2	40	169.9 ± 6.60	0.17 ± 0.02	-12.8 ± 3.42
10	5	25	-	2	2	0.5	-	2, 10/2, 40	10000	5	2.5	10/2	40	219.4 ± 7.82	0.23 ± 0.01	-22.0 ± 3.94
11	5	25	-	2	2	0.5	-	2, 10/2, 40	10000	5	5	10/2	30	171.1 ± 0.7	0.12 ± 0.03	-18.7 ± 1.90
12	5	25	-	2	2	0.5	-	2, 10/2, 40	10000	5	5	5/2	40	183.3 ± 5.49	0.20 ± 0.03	-10.5 ± 1.66
13	5	25	-	2	2	0.5	5%	2, 10/2, 40	10000	5	5	10/2	40	161.1 ± 6.30	0.15 ± 0.04	-1.47 ± 0.35
14	5	25	-	2	2	2	5%	2, 10/2, 40	10000	5	5	10/2	40	171.9 ± 4.61	0.25 ± 0.04	-1.42 ± 0.60
15	5	25	-	2	2	0.5	-	1, 10/2, 40	10000	5	5	10/2	40	177.3 ± 1.26	0.20 ± 0.02	-18.5 ± 0.95
16	5	25	-	2	2	0.5	-	2, 10/2, 30	10000	5	5	10/2	40	183.6 ± 16.53	0.23 ± 0.02	-18.8 ± 1.18
17	5	25	-	1	2	0.5	-	2, 10/2, 40	10000	5	5	10/2	40	176.3 ± 8.37	0.18 ± 0.04	-23.7 ± 0.25
18	5	25	-	2	2	0.5	-	2, 10/2, 40	10000	5	No Sonication			647.2 ± 114.19	0.90 ± 0.01	-32.1 ± 0.44
19	5	25	5	2	2	0.5	-	2, 10/2, 40	10000	5	-	-	-	470.80 ± 7.89	0.54 ± 0.03	24.17 ± 1.16
20	5	25	5	2	2	0.5	-	2, 10/2, 40	10000	10	-	-	-	309.70 ± 13.75	0.33 ± 0.03	17.70 ± 1.11
21	5	25	5	2	2	0.5	-	2, 10/2, 40	10000	10	5	10/2	40	275.93 ± 3.52	0.44 ± 0.02	30.17 ± 1.80
22	5	25	5	2	2	0.5	-	2, 10/2, 40	10000	5	5	10/2	40	162.93 ± 13.81	0.23 ± 0.04	22.50 ± 2.94

A: Epigallocatechin 3-gallate; **B:** Poly(lactic-co-glycolic acid) 50:50); **C:** Octadecylamine; **D:** Dichloromethane; **E:** PVA conc. for primary emulsion (% w/v); **F:** PVA conc. for secondary emulsion (% w/v); **G:** Sodium chloride (% w/v); **H:** Probe sonication parameters for primary emulsion preparation; **I:** High speed homogenization parameters for secondary emulsion preparation; **J:** Probe sonication parameters for secondary emulsion preparation; **K:** Particle size (nm); **L:** Polydispersibility index; **M:** mucoadhesive strength (mV)

The optimized formulation was lyophilized using Christ Freeze-dryer ALPHA 1-2 LDplus at 10 mTorr pressure and −48°C for 48 h. for solid-state characterization [22]. The HNC formulation was prepared by dispersing the Carbopol-980 as a mucoadhesive agent on the nanoparticles dispersion using a mechanical stirrer, and the pH was adjusted with triethanolamine [11].

The nanoparticle was evaluated for encapsulation efficiency, particle size, zeta potential, polydispersibility index, morphological evaluation (transmission electron microscopy, TEM), solid-state characterization such as differential scanning calorimetry (DSC), Fourier-transform infrared spectroscopy (FTIR), and X-ray crystallography (XRD). HNC formulation was evaluated for pH examination, viscosity, spreadability and rheological behaviour, EGCG content uniformity, thermodynamic stability, and mucoadhesive strength study. *In vitro* EGCG release and diffusion study were performed using a dialysis membrane, while porcine buccal mucosa was utilised for evaluating its permeation and retention using *ex vivo* studies. Both *in vitro* and *ex vivo* studies were performed using Franz diffusion cell apparatus and simulated saliva media (pH 6.75) as release media and evaluated for the presence of EGCG in the collected samples [11, 23]. The optimized formulations were evaluated for their stability at accelerated temperature and humidity conditions for a duration of 6 months.

The efficacy and safety of the formulations were evaluated in an *in vivo* model of OSF induced using an extract of areca nut in Sprague Dawley rats. The Institutional Animal Ethical Committee (Kasturba Medical College, MAHE, Manipal) approved the protocol (#IAEC/KMC/112/2018). CPCEA (Committee for the Purpose of Control and Supervision of Experiments on Animals) guidelines were followed for animal experiments. The schematic representation for OSF induction and treatment is shown in Fig. 2. Sub-buccal injection of (100 μL, 20 mg/mL) ANE was given at left buccal mucosal tissue of rats for induction of OSF for 2 months, followed by treatment of disease-induced rats with optimized formulations [9, 24]. The standard treatment was betamethasone injection (BTM Inj.), pure EGCG hydrogel, and EGCG HNC formulations, and normal rats in the control group were compared with the disease-induced control rats. GraphPad Prism 8.0.2 statistical software was used to assess the results using one-way ANOVA ($P<0.05$).

Results

Physical Characteristics of Octadecylamine-Modified PLGA Nanoparticles

Table I represents the different physical properties assessed for octadecylamine-modified PLGA nanoparticles. Based on preliminary trials, it was inferred that the material and processing parameters have an important role in obtaining the desired particle size, zeta potential, and polydispersibility index (PDI); hence, these parameters were considered further during preparation and evaluation.

Fig. 2 Study design and schematic representation for oral submucous fibrosis (OSF) induction and treatment planner. OSF was induced in Sprague Dawley rats by sub-buccal injection of areca nut extract (ANE) (100 μL, 20 mg/mL) on alternative days for 60 days (2 months). The treatment with the standard drugs and the newer formulation, EGCG HNC was applied for 45 days after the induction period. Treatment continued for 90 days to observe its safety
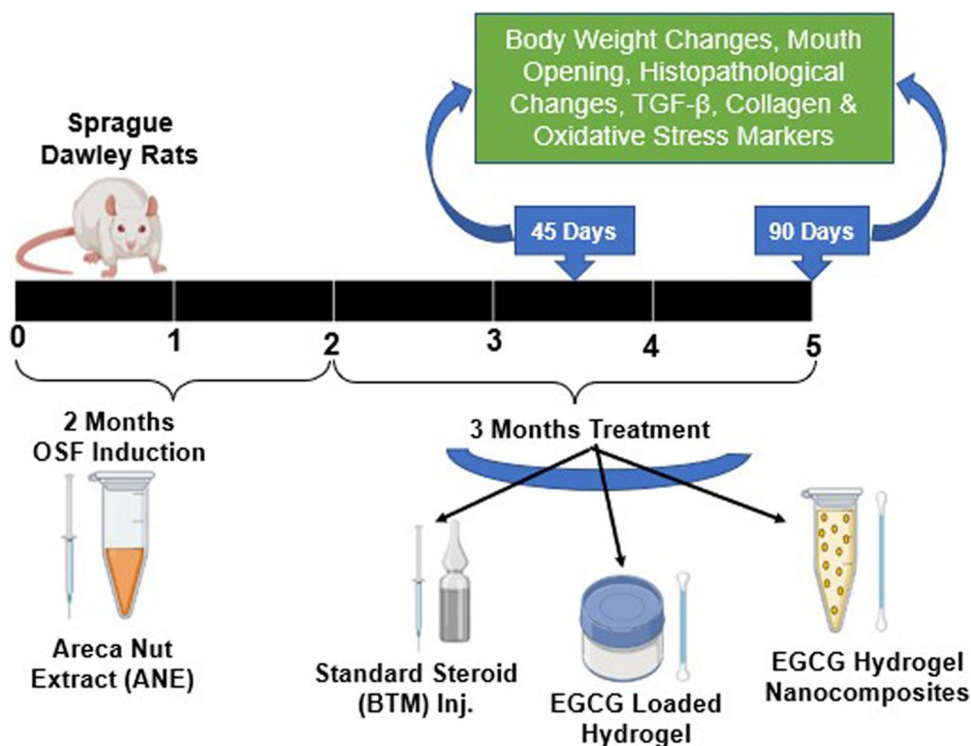
Effect of PLGA and PVA on Particle Size, PDI, and Zeta Potential

An increase in PLGA concentration from 25 to 50 mg, increased the particle size and PDI while zeta potential decreased (trial 2, trial 4). The increase in PVA concentration (1 to 2%) decreases the particle size (trial 2, trial 8) in primary emulsion. The rise in concentration of PVA from 0.5 to 2% (trials 2 and 3) increased the particle size and PDI during secondary emulsion while zeta potential decreased. Hence, 0.5% concentration was selected for the secondary emulsion preparation. The zeta potential was negative for the unmodified PLGA nanoparticles and positive for the modified PLGA nanoparticles due to the carboxyl group at the terminal end of nanoparticle surface [25, 26].

Effect of Dichloromethane on Particle Size, PDI, and Zeta Potential

It was observed that the increase in dichloromethane (DCM) volume during the preparation of primary emulsion leads to a decrease in particle size, PDI, and zeta potential (trials 2 and 17, Table I).

Effect of Sodium Chloride on Particle Size, PDI, and Zeta Potential

With the addition of sodium chloride, the encapsulation efficiency was found to be almost the same while there was slightly increase in particle size and PDI whereas drastic decrease in zeta potential (trials 2 and 13, trials 3 and 14; Table I) due to the possible neutralization, so further trials were not considered [27, 28].

Effect of Homogenization (HSH) Speed and Time on Particle Size, Zeta Potential, and PDI

Based on the obtained results, it can be concluded that with the increase in homogenization time and speed, there was not much difference, but the homogenization to some extent can help to reduce the particle size after that, it will not affect any responses (trials 2, 5, 6, and 7; Table I).

Effect of Sonication Parameters (Amplitude, Pulse, and Time) on Particle Size, PDI, and Zeta Potential

Based on the comparison between trial 2 with trials 9–12, trial 15, and trial 16 (Table I), the sonication amplitude, time,

and pulse increase, and the particle size and PDI decrease while the increase in the zeta potential was observed.

Effect of Octadecylamine Addition on PDI, Particle Size, and Zeta Potential

The addition of octadecylamine to the formulation showed no or negligible particle size change, whereas increased PDI within the limit while the particle charge shifted from negative to positive (trials 2 and 22; Table I). There was an increase in homogenization time and speed, leads to an increase in the zeta potential, particle size, and PDI (in trials 21 and 22; Table I). The sonication of formulation reduced particle size and PDI while there was not much effect on zeta potential (trials 19 and 22; Table I).

Evaluation Results of Octadecylamine-Modified PLGA Nanoparticles

The octadecylamine-modified nanoparticles had the highest encapsulation efficiency (38.71 ± 6.11%) as compared to unmodified nanoparticles (23.76 ± 2.82%). Both nanoformulations (unmodified and modified) showed the retention of the pure EGCG characteristic peaks, and no or negligible shift in the EGCG FTIR spectral bands in the case of the formulation was observed (Fig. 3a). A sharp melting endothermic peak was observed at 226.54°C by pure EGCG (Fig. 3b), which confirms the EGCG identity and crystallinity. The disappearance of EGCG endothermic peak in formulations indicates that the EGCG crystallinity converted to amorphous form or solid solution state in PLGA nanoparticles (Fig. 3b). The XRD pattern (Fig. 3c) of pure EGCG had defined sharp peaks at 2Ø angles such as 15.51°, 16.86°, 20.64°, 21.45°, 22.44°, 24.46°, 25.78° and 29.06° which confirms the crystalline nature of the EGCG which was reduced in case of nanoparticles such as unmodified nanoparticles (16.98° and 22.88°) and modified nanoparticles (22.50°) thus indicates transformation of EGCG crystalline nature to amorphous nature upon preparing its nanoparticle formulations. The results are similar to that of a previous study on EGCG-encapsulated albumin nanoparticles [29]. The surface morphology of modified EGCG-PLGA nanoparticles was spherical, smooth-shaped, and had a uniform distribution in dispersion. FTIR spectrum, DSC thermogram, and XRD graph of EGCG, octadecylamine-modified EGCG-PLGA, and unmodified EGCG-PLGA nanoparticles are shown in Fig. 3a, b, and c, respectively. The morphological analysis of modified nanoparticles is shown in Fig. 3d.

Evaluation and Characterization of Hydrogel Nanocomposite

The pH of optimized HNC prepared with Carbopol-980 was neutral (between 6 and 6.75), indicating no or negligible
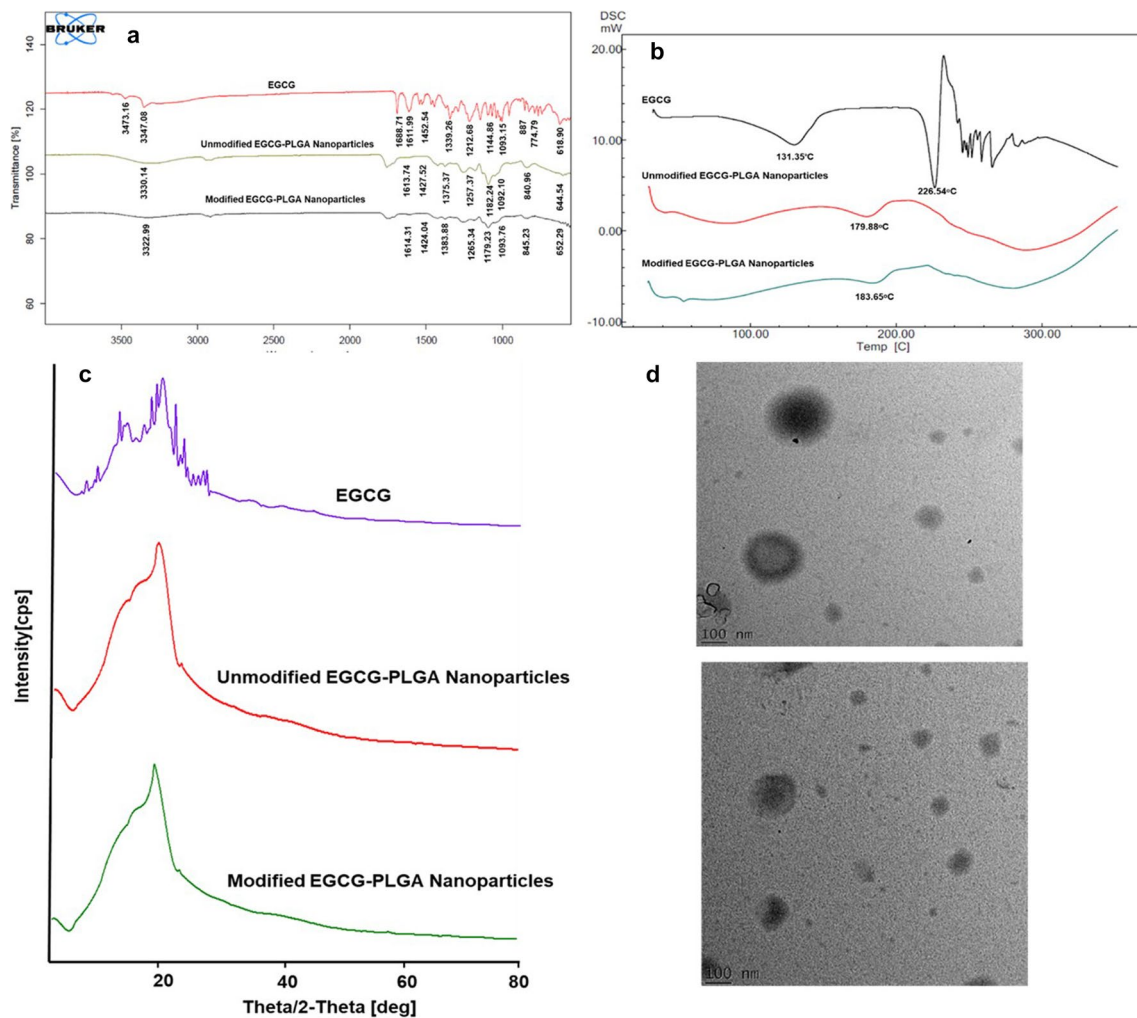
Fig. 3 Characterization of pure EGCG, unmodified EGCG-PLGA nanoparticles and modified EGCG-PLGA nanoparticles. **a**: FTIR; **b**: DSC; **c**: XRD; **d**: Morphological analysis by TEM in two specimens

chances of irritation in the mucosa. The viscosity, spreadability, and mucoadhesiveness are prime requirements for buccal drug delivery.

The viscosity and spreadability of different modified HNC formulations of 1%, 2%, and 3% w/v gelling agent concentration were found to be 6810.43 ± 77.27 Cps, 14378 ± 84.56 Cps, 0.89 ± 0.02 Cps at 25°C and 1.46 ± 0.01 g-cm/s, 1.09 ± 0.01 g-cm/s, 0.89 ± 0.02 g-cm/s, respectively. The optimized HNC passes the thermodynamic stability, which indicates the stability over centrifugation and freeze-thaw study [11, 30]. The gelling agent 1% w/v Carbopol-980 was easily spreadable and not much viscous; hence, the same concentration was used for further evaluation. The mucoadhesiveness of different modified HNC formulations of 1%, 2%, and 3% w/v gelling agent concentration were found to be 0.40 ± 0.002N, 1.1 ± 0.001N and 2.1 ± 0.0003N, respectively. The graphical representation of time (min) *versus* load (N) for mucoadhesiveness of optimized HNC is shown

in Fig. 4a, b, and c. The results of rheological behaviour indicate that the optimized HNC formulation showed shear thinning or pseudoplastic flow (Fig. 4d, e, and f), which implies that the viscosity increases upon a decrease in shear rate [11, 23]. The unmodified hydrogel formulations showed $84.43 \pm 16.36\%$ EGCG content, and the modified hydrogel had $81.67 \pm 19.17\%$.

In Vitro EGCG Release from the Hydrogel Formulations and Its Diffusion

The graphical representation of *in vitro* release and diffusion studies are shown in Fig. 5A. The pure EGCG solution had 100% release within 4 h, while EGCG-loaded PLGA nanoparticles and octadecylamine-modified EGCG loaded PLGA nanoparticles dispersion showed EGCG release in sustained or controlled manner, $49.07 \pm 1.64\%$ and $44.42 \pm 1.01\%$, respectively at the end of 24 h.
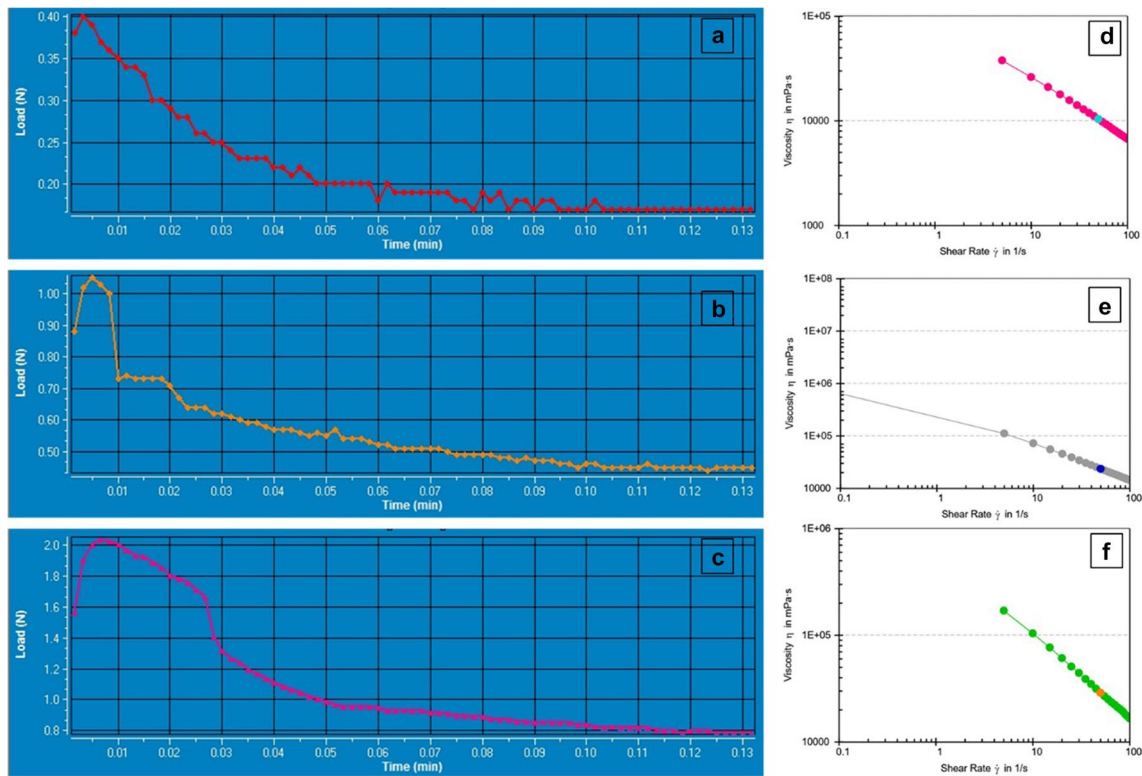
Fig. 4 Evaluation hydrogel nanocomposite (HNC) for mucoadhesiveness (**a** 1%; **b** 2%; **c** 3% w/w Carbopol-980) and rheology (**d** 1%; **e** 2%; **f** 3% w/w Carbopol-980). **d**, **e**, and **f** indicate shear thinning or pseudoplastic flow, increase in viscosity as the shear rate decreases
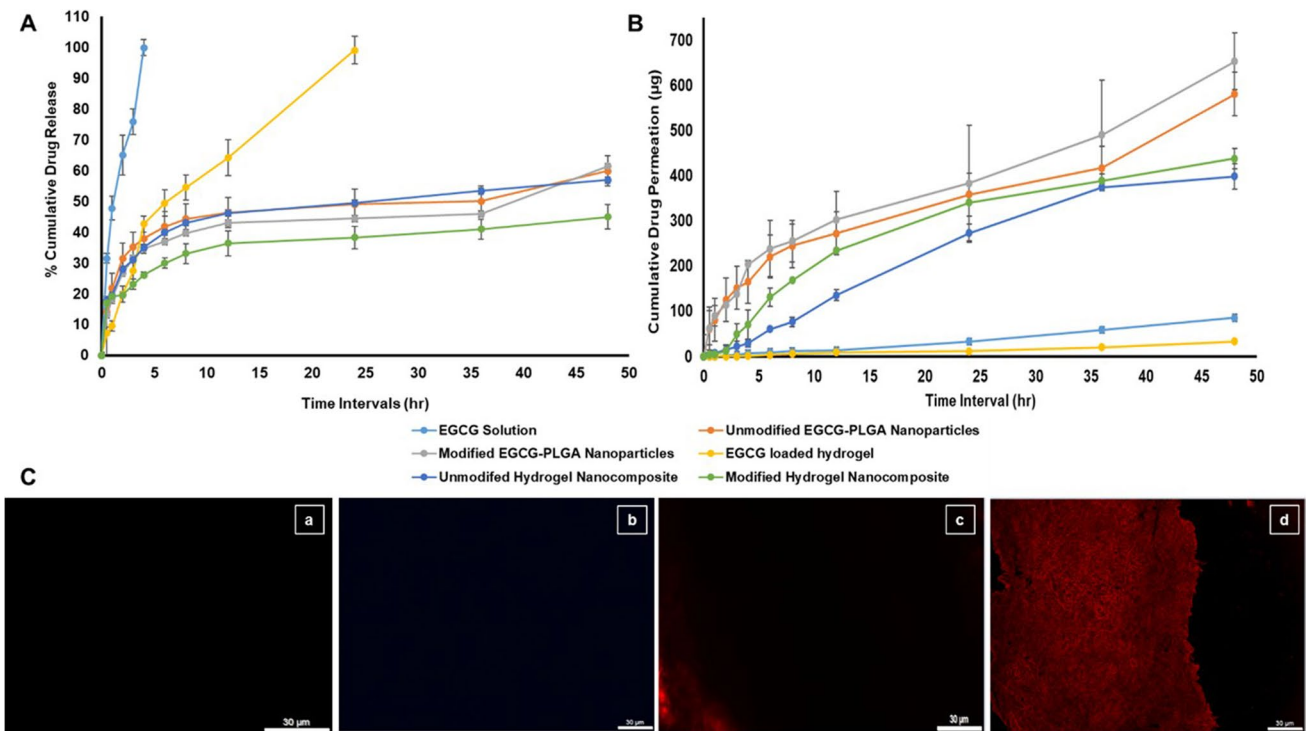

Fig. 5 EGCG release from hydrogel formulations and permeation studies. **A** *In vitro* EGCG release; **B**: *Ex vivo* permeation studies; **C**: *Ex vivo* retention studies of fluorescent-tagged nanoparticles through the buccal mucosal membrane (*a*: Control skin; *b*: Rhodamine solution on the skin; *c*: Fluorescent tagged unmodified PLGA nanoparticles; *d*: Fluorescent tagged modified PLGA nanoparticles)

In vitro diffusion or permeation study also followed a similar release pattern. The pure EGCG-loaded hydrogel showed faster release than the HNC-loaded EGCG encapsulated PLGA nanoparticles and octadecylamine-modified PLGA nanoparticles as polymer and gelling agent barrier restrict the release of EGCG from HNC. The EGCG release results compared the EGCG solution and the surface-modified and unmodified nanoparticles release. There was no significant difference observed in the results; however, the release behaviour of unmodified and modified nanoparticles are significant. For HNC, a statistically significant difference was observed between the comparative groups, such as EGCG-loaded hydrogel *vs.* unmodified HNC, EGCG-loaded hydrogel *vs.* modified HNC, and modified HNC *vs.* unmodified HNC. The data related to the kinetics models plotted is shown in Table II. The *in vitro* EGCG release and Higuchi model, followed by diffusion samples with the highest r^2 value, confirmed that the diffusion control mechanism plays a major role in the release of EGCG. Except for the EGCG solution and EGCG loaded hydrogel, all showed n value less than 0.45, which indicates the Fickian diffusion mechanism, while both showed anomalous non-Fickian transport (both diffusional and relaxational transport) [31, 32].

Ex Vivo Permeation and Retention Studies

EGCG solution and its hydrogel exhibited permeation of 33.09 ± 25.88 and 11.97 ± 0.81 µg, respectively, through the buccal mucosa at the end of 24 h. At the end of 24 h, the octadecylamine-modified nanoparticles had faster and higher permeation (383.60 ± 67.40 µg) than the unmodified nanoparticles (358.16 ± 128.23 µg). The octadecylamine-modified nanoparticles loaded HNC showed faster permeation (340.47 ± 2.42 µg) than the unmodified nanoparticles loaded HNC (273.11 ± 20.19 µg). In multiple comparisons of one-way ANOVA analysis, when the results of *ex vivo* permeation of EGCG from nanoparticles were compared with the pure EGCG solution, a statistically significant difference ($p<0.05$) was observed. However, there was no significant difference between the unmodified and modified nanoparticles. A significant difference ($p<0.05$) was observed between the EGCG-loaded hydrogel compared with the unmodified and modified HNC and also between the unmodified and modified hydrogel system. The mathematical kinetics model data is shown in Table II.

As per the results obtained, the *ex vivo* EGCG permeation followed zero-order release kinetics due to its higher r^2 values. All groups showed n value of more than 0.45, indicating anomalous non-Fickian transport (diffusional and relaxational transport) [31]. The comparative permeation behaviour of nanoparticles and its loaded hydrogel is shown in Fig. 5B. The permeation and retention behaviour of modified and unmodified PLGA nanoparticles tagged with a fluorescent probe, rhodamine B through porcine buccal mucosa were compared. There was a successful permeation of octadecylamine-modified EGCG encapsulated PLGA nanoparticles tagged with rhodamine B compared to pure rhodamine solution and unmodified EGCG encapsulated PLGA nanoparticles tagged with rhodamine B. The higher permeation of octadecylamine-modified nanoparticles through the buccal mucosal membrane was observed, which could be due to the formation of nanoparticle interconnections with positive charge nanoparticles and buccal membrane with negatively charged and also nanosize of the

Kinetics or release mechanism models	Zero order		First order		Higuchi model		Kores-peppas model		
	r^2	K_0	r^2	K_1	r^2	K_H	r^2	n	K_{KP}
In vitro release data of EGCG									
EGCG solution	0.96	27.15	0.81	0.65	0.99	47.00	0.98	0.52	0.46
Unmodified EGCG-PLGA nanoparticles	0.87	7.34	0.74	0.30	0.98	18.01	0.95	0.41	0.22
Modified EGCG-PLGA nanoparticles	0.87	6.54	0.74	0.29	0.99	16.03	0.95	0.41	0.19
EGCG-loaded hydrogel	0.97	7.98	0.83	0.30	0.98	18.41	0.95	0.80	0.12
Unmodified HNC	0.88	6.93	0.74	0.29	0.99	16.96	0.99	0.34	0.22
Modified HNC	0.85	5.26	0.72	0.27	0.97	12.99	0.93	0.23	0.19
Ex vivo EGCG permeation data									
EGCG solution	0.98	0.15	0.01	-0.04	0.90	0.32	0.75	3.10	0.00
Unmodified EGCG-PLGA nanoparticles	0.94	7.31	0.77	0.30	0.99	17.37	0.99	0.51	0.17
Modified EGCG-PLGA nanoparticles	0.94	7.77	0.77	0.30	0.99	18.43	0.96	0.49	0.18
EGCG-loaded hydrogel	0.92	0.06	0.25	-0.12	0.76	0.14	0.89	0.99	0.00
Unmodified HNC	0.99	0.61	0.65	0.08	0.89	1.34	0.98	1.00	0.00
Modified HNC	0.97	1.33	0.74	0.13	0.84	2.86	0.98	1.44	0.00

Table II Mathematical Models for *In Vitro* Release and *Ex Vivo* Permeation of EGCG

EGCG, epigallocatechin 3-gallate; *PLGA*, poly(lactic-co-glycolic acid); *HNC*, hydrogel nanocomposite

nanoparticles providing equal contribution in efficient permeation of nanoparticles through different layers of buccal mucosal membrane. The comparative permeation behaviour of nanoparticles is shown in Fig. 5C.

Stability Studies at Accelerated Conditions

The accelerated stability studies confirmed the stability of mucoadhesive HNCs over 6 months as least changes were observed in the pH, appearance (texture), weight loss, and viscosity of HNC. After evaluation of the presence of EGCG in mucoadhesive HNC of stability samples, no or negligible changes were observed in the EGCG content when compared to the initial samples (0th day) [16, 33].

Efficacy and Safety Studies in Rats

In Vivo Efficacy Studies

Optimized formulations and the BTM Inj. (standard treatment), were evaluated for their efficacy using an *in vivo* ANE-induced OSF rat model. There was no mortality in rats during OSF induction and the treatment period. Reduction in mouth opening and histopathological changes indicate the induction of OSF (Fig. 6a, b, and c). At the end of 3 months

(treatment period) there was no significant change in the bodyweight of rats (Fig. 6a), while a significant increase in mouth opening was observed in the HNC formulation-treated rats (Fig. 6b). The OSF-induced rats had a decrease in epithelial thickness (44.66 ± 36.48 μm), while formulation-treated rats [BTM Inj. − 67.51 ± 11.28 μm, EGCG (40.91 mg/kg) − 54.06 ± 12.46 μm, EGCG (81.81 mg/kg) − 76.02 ± 34.76 μm, EGCG-HNC (40.91 mg/kg) − 67.01 ± 16.55 μm, and EGCG-HNC (81.81 mg/kg) − 85.09 ± 32.39 μm] showed significant improvement or enhancement in epithelial thickness compared to the control (183.83 ± 29.29 μm) and OSF-induced rats (44.66 ± 36.48 μm). The rats treated with 81.81 mg/kg did not change their body weight and improved mouth opening compared to the 40.91 mg/kg dose. Further, the histopathology confirmed that a 40.91 mg/kg dose was ineffective in improving the OSF condition in rats. Therefore, dose 2 (81.81 mg/kg dose) was considered for further evaluation.

Histopathology of oral mucosa in rats of the control group had 10–16 layers of thickness stratified squamous keratinized epithelium with rete ridges, connective tissue beneath the epithelium shows few blood vessels and muscle fibers while OSF-induced rats had 3–6 layered thick ulcerative epithelium with the presence of scab which showed fibrin and cell debris, the large necrosed area in the dermis,
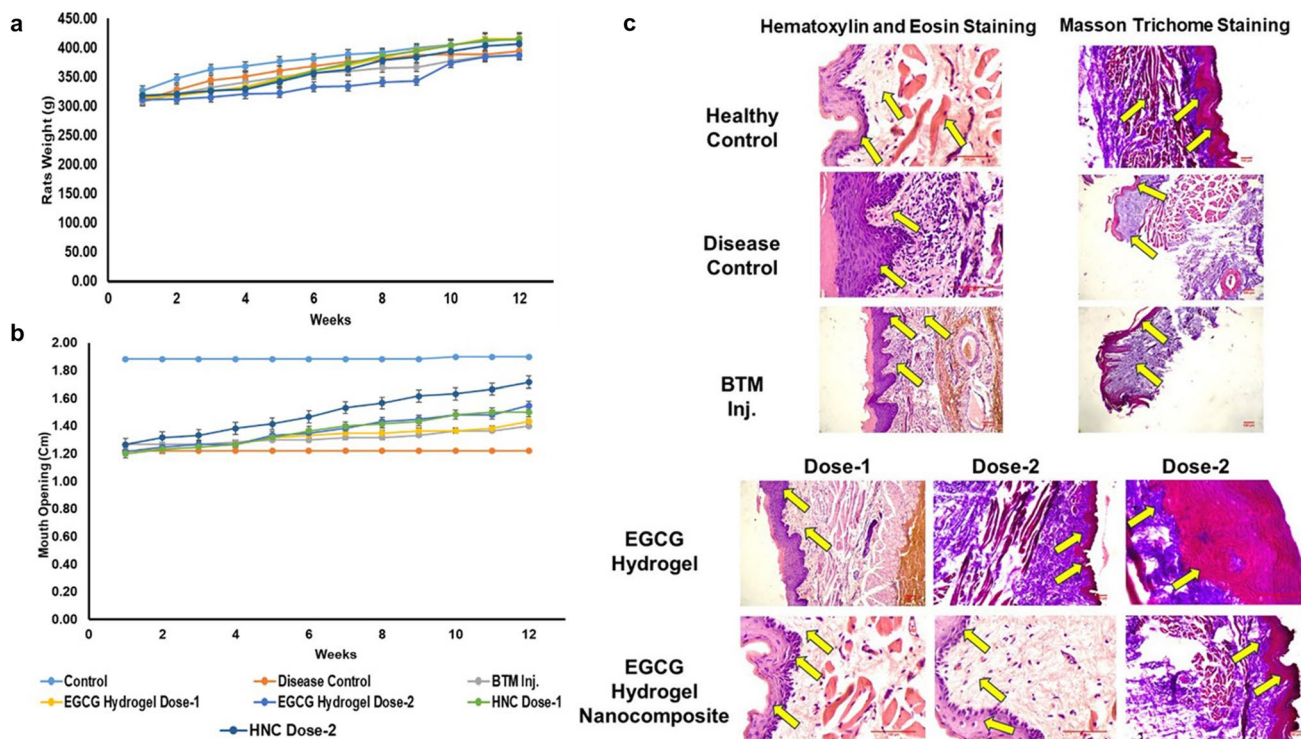

Fig. 6 *In vivo* efficacy studies of EGCG-hydrogel composites (HNC) in areca nut extract (ANE)-induced rat-OSF model. Parameters of evaluation include body weight (*a*), mouth opening (*b*), and histo-pathological characterization (*c*) of different treatments; EGCG: Epigallocatechin 3-gallate; BTM Inj.: Betamethasone injection; Histopathological images were captured at a magnification of ×100

granulomatous inflammation with giant cells, an abundance of chronic inflammatory cells like lymphocytes, congested blood vessels. The rats treated with BTM Inj. had atrophic epithelium with 3–6 layers thickness, the connective tissue beneath the epithelium has dense infiltration of lymphocytes, muscle fibers, and mild fibrosis areas were seen while pure EGCG treated rats showed stratified squamous epithelium consisting of 3–6 cell layers with an atrophic region. Also, the absence of rete ridges was seen in the epithelium, and lymphocytic infiltrates, congested blood vessels, and many macrophages were seen in the dermis. Fibrosed areas are seen in the dermis [9]. The submucous histopathology of rats treated with HNC had an increase in epidermis thickness nearer to healthy rats (6-10 layers) with rete ridges on the epithelium membrane. The connective tissue beneath the epithelium was congested blood vessels and muscle fibers with very few lymphocytes.

Upon Masson trichrome staining, the submucous histopathology of OSF-induced rats had a tight collagen fibre arrangement in buccal mucosa which was loosely arranged in control rats. BTM Inj. EGCG- and EGCG hydrogel–treated rats indicated a presence of tightly collagen fibre arrangement, while the nanoformulation loaded hydrogel (HNC) treated group showed a significant reduction in the collagen concentration [9]. The histopathological images of the buccal mucosa by H&E staining and Masson trichome staining are shown in Fig. 6c (The original images of histopathological studies are provided in the supplementary file).

OSF-induced rats had an increase in serum collagen type-1 and TGF-β1 in comparison to control group rats [34, 35]. The formulations treated groups showed a significant reduction in collagen type-1 and TGF-β1 compared to OSF-induced rats, indicating the recovery from the OSF condition. A significant difference was observed between the rats in treatment groups when compared to the disease group, such as the disease control group *versus* BTM Inj., disease control group *versus* EGCG hydrogel, EGCG hydrogel, and disease control group *versus* HNC for the concentration of collagen and TGF-β [9]. The plots of collagen and TGF-β1 *versus* different groups are shown in Fig. 7.
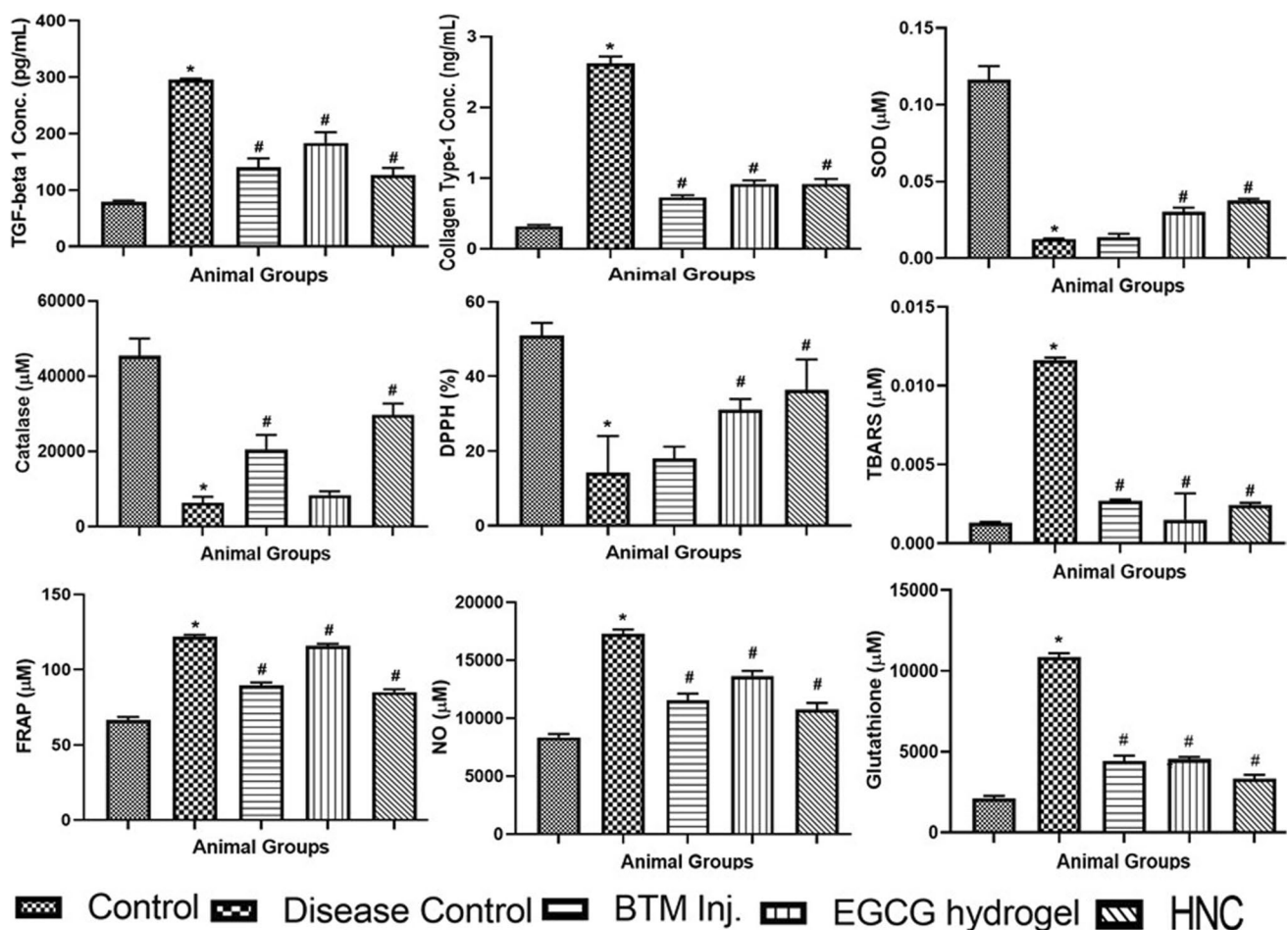

Fig. 7 Serum TGF-β1, collagen type-1, and biochemical assays. BTM Inj. – Betamethasone injection, HNC – Hydrogel Nanocomposite; *$p<0.0001$ compared to control group, #$p<0.0001$ compared to disease control group.

The endogenous antioxidants get disturbed due to the presence of free radicals [36, 37]. Similar results were observed in this study. An increase in glutathione, TBARS, FRAP, and NO concentrations (Fig. 7) was observed in OSF rats in comparison to healthy rats. A significant reduction in NO, TBARS, FRAP, and glutathione was observed upon treatment with the standard BMT-inj and the HNC formulations. The reduction in %DPPH, catalase, and SOD (Fig. 7) was observed in the disease-induced rats in comparison to control rats. A statistically significant difference in SOD and DPPH scavenging was observed between EGCG hydrogel treatment and EGCG HNC, except for BTM Inj. The catalase significantly increased upon treatment compared with the OSF-induced rats except for pure drug (EGCG) treated rats. Among all formulations, HNC formulations showed better improvement in disease conditions compared with the OSF-induced rats, which was reflected in histopathology, antioxidant assays, and TGF-β1 and collagen type-1 [9].

Results of *in vivo* Safety Studies

There were no noticeable changes in collected organs and buccal mucosa from the treated rats by visual observation; this was also confirmed by performing histopathology [9]. The buccal mucosal tissue collected from other groups did not show any histopathological changes in the buccal

mucosal region, which indicates the safety of HNC formulations except standard BTM Inj. as it showed little swelling or infection at the injection site, and literature proved the same [38–40]. All treated rats had proper liver histopathology lobule arrangement with the presence of central vein and portal triads, numerous sinusoids with liver cells, and dilated or congested blood vessels with mild infiltration of chronic inflammatory cells like lymphocytes while no necrosis and degenerative changes were observed upon any treatment. None of the treatments had any changes in kidney histopathology. No inflammation or degeneration and no necrosis changes in the kidney were observed in any of the treated rats. The comparative histopathological images of the buccal mucosa, liver, and kidney of rats in different treatment groups are shown in Fig. 8 (The original images of histopathological studies are provided in the supplementary file).

There was an increase in urea and creatinine in rats with OSF, EGCG hydrogel, and BTM Inj. groups, while the HNC-treated group exhibited urea and creatinine within the normal. The OSF- rats had an increased AST and ALT in serum, while a statistically significant reduction of both was observed upon HNC treatment, compared to standard treatment (BTM Inj.) and pure EGCG hydrogel [41, 42]. The comparative graphs of various biochemical assays with different animal groups are shown in Fig. 8.
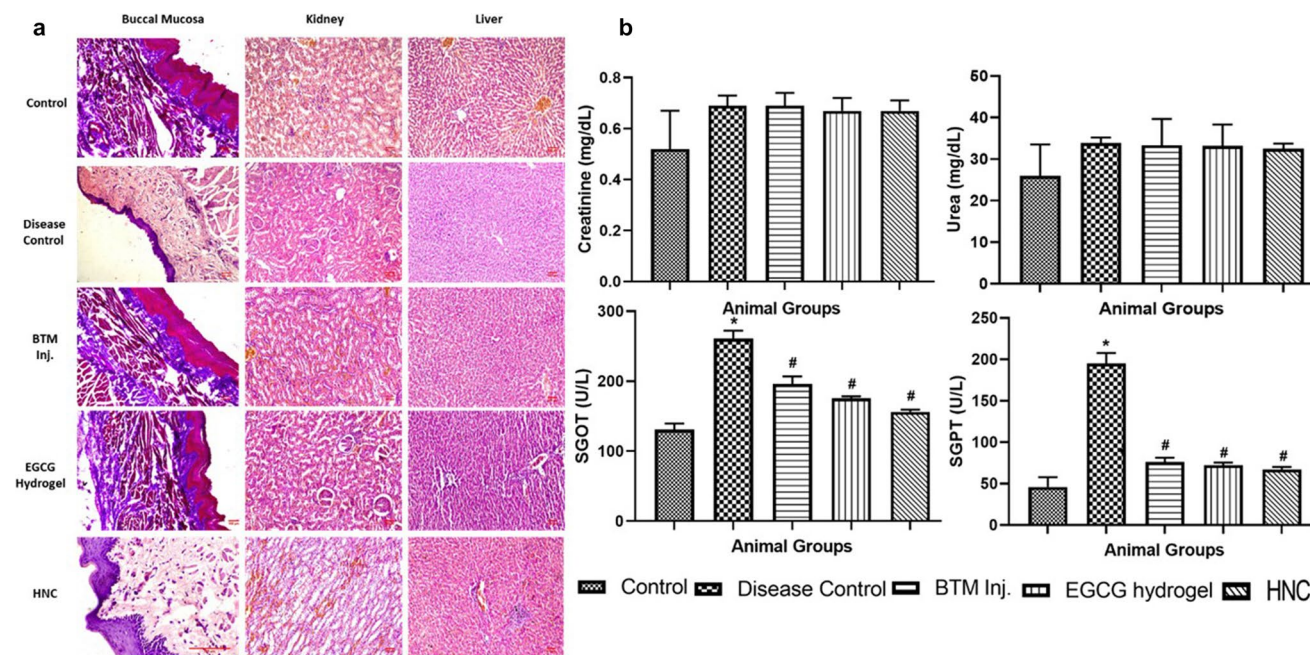

Fig. 8 *In vivo* safety of EGCG hydrogel nanocomposite (HNC) in OSF-induced rats. *a*: Histopathology of buccal mucosa, liver, and kidney; *b*: Serum biochemical parameters; EGCG: Epigallocatechin 3-gallate; BTM Inj.: Betamethasone injection; *p<0.0001 compared to the control group, # p<0.0001 compared to the disease control group; Histopathological images were captured at a magnification of ×100

Discussion

The process- and material-related parameters were considered for formulation and optimization of formulation and evaluated for their effect on responses such as particle size, PDI, and zeta potential. An increase in PLGA concentration increases dispersed phase viscosity, resulting in improper PLGA dispersibility in the aqueous phase, while the generation of high shear forces due to high viscous resistance during emulsification, leading to the formation of coarse particles of larger size during the diffusion method and sometimes larger particles are formed or formation of coacervates [43, 44]. In the case of primary emulsion, a decrease in particle size was observed, could be due to narrower of granulometric distribution and emulsifier stabilizing function. Insufficient stabilizer also leads to the formation of larger particles by forming aggregates [44, 45]. An increase in DCM content increases the solvent front kinetic energy, followed by a uniform distribution of droplets in the aqueous phase, which forms smaller nanoparticles due to the high diffusion rate [43, 46].

An increase in sonication parameters releases higher energy during sonication, which leads to a speedy reduction in granulometric distribution due to the rapid formation of nanodroplets from polymeric dispersion (organic phase), decreasing the particle size and PDI while increasing the zeta potential. The obtained results are in accordance with previous study results [47, 48]. The addition of octadecylamine in the formulation increases the encapsulation efficiency which may be due to the presence of more surface area for encapsulating EGCG [49].

The concentration of polymer is directly proportional to viscosity and mucoadhesiveness while inversely proportional to spreadability. The viscosity and mucoadhesive increases due to an increase in the concentration of polymer while spreadability decreases. The hydrophilic nature of EGCG and its affinity towards the aqueous media helped release 100% within 4 h from hydrogel, while due to encapsulation of EGCG inside the nanoparticle carrier, it shows controlled or sustained release of EGCG due to the presence of a tight polymer barrier [29, 50].

Permeation of EGCG from its solution and hydrogel shows slower permeation, which may be due to the hydrophilic nature of the pure EGCG to the permeation and poor affinity towards the lipophilic buccal mucosal membrane and the higher particle size of the EGCG molecules can be difficult to permeate through the buccal mucosa. The modified nanoparticles and its hydrogel showed faster permeation due to the creation of contacts in the middle of nanoparticles with positively charged and buccal membranes than with negatively charged [51–53]. One research study performed by Roblegg and his team showed that the nanoparticles with positive charge (cationic, 200 nm) and negative charge (anionic, less than 20 nm) can permeate faster the buccal mucosal membrane with ease [17, 51, 54]. The *ex vivo* permeation and retention study showed the higher permeation of octadecylamine-modified nanoparticles through buccal mucosal membrane was observed which could be due to the formation of interconnections among the nanoparticles with a positive charge and buccal membrane with negatively charged and also nanosize of the nanoparticles provides an equal contribution in permeation of nanoparticles through different layers of buccal mucosal membrane efficiently [11].

In vivo there was a significant improvement in disease condition by improving the mouth opening condition, a significant reduction in collagen and TGF-β1, improvement in epidermal thickness, and antioxidants. Generally, the nanosized particles with positive charges can permeate the membrane faster, which was also proved by the *ex vivo* studies performed. Nanoparticles have the special advantage of permeation, retention, and showing their therapeutic action at the desired site or disease site in the buccal membrane [55, 56]. Based on these results obtained from the safety study, it was observed that the developed and optimized formulation did not show any toxicity to the vital organs and buccal mucosa, which indicates that the formulation can be used safely for the treatment of OSF.

Conclusion

The surface-modified nanoparticles with positively charged octadecylamine improved buccal membrane permeation. The optimized formulation showed the required properties, specifically mucoadhesiveness, controlled release of EGCG from HNC formulation, and stability for a longer time. In the OSF rat model, EGCG formulations decreased TGF-β1 and collagen concentration. The histopathology study and biochemical parameters proved to improve disease conditions. The HNC formulation was safer on the buccal mucosal membrane, liver, and kidney upon a longer treatment period. Thus, the developed and optimized HNC formulation is safer, non-toxic, and efficient and therefore can be used as an alternative treatment strategy for OSF therapy.

Author's Contribution Chetan Hasmukh Mehta: conceptualization, data curation, formal analysis, methodology, validation, visualization, writing original draft. Varalakshmi Velagacherla: sample analysis

and data curation. Suman Manandhar: sample analysis and data curation. Yogendra Nayak: conceptualization, methodology, supervision, resources, data analysis, and manuscript writing review and editing. K. Sreedhara Ranganath Pai: supervision, manuscript review and editing. Shruthi Acharya: resources, supervision, manuscript review and editing. Usha Yogendra Nayak: conceptualization, methodology, project administration, resources, supervision, data analysis, manuscript review and editing. All contributing authors have approved the final version of the manuscript.

Data Availability The generated datasets during and/or analyzed during the current study is included in the manuscript and available from the corresponding author on reasonable request.

Declarations

Competing Interests The authors declare no competing interests.

Ethical Approval Animals were treated ethically according to the protocol of the ethics committee of Kasturba Medical College, MAHE, Manipal (#IAEC/KMC/112/2018).

References

1. Qin X, Ning Y, Zhou L, Zhu Y. Oral submucous fibrosis: etiological mechanism, malignant transformation, therapeutic approaches and targets. Int J Mol Sci. 2023;24:4992. https://doi.org/10.3390/ijms24054992.

2. Sharma M, Shetty SS, Radhakrishnan R. Oral submucous fibrosis as an overhealing wound: Implications in malignant transformation. Recent Pat Anticancer Drug Discov. 2018;13:272–91. https://doi.org/10.2174/1574892813666180227103147.

3. Chen X, Xie H, Guo J. Drug treatment for oral submucous fibrosis: an update. BMC Oral Health. 2023;23:48. https://doi.org/10.1186/s12903-023-03488-9.

4. Arakeri G, Rai KK, Boraks G, Patil SG, Aljabab AS, Merkx MAW, Carrozzo M, Brenhan PA. Current protocols in the management of oral submucous fibrosis: an update. J Oral Pathol Med. 2017;46:418–23. https://doi.org/10.1111/jop.12583.

5. Zhang P, Chua NQE, Dang S, Davis A, Chong KW, Zhang P, et al. Molecular mechanisms of malignant transformation of oral submucous fibrosis by different betel quid constituents—does fibroblast senescence play a role? Int J Mol Sci. 2022;23:1637. https://doi.org/10.3390/ijms23031637.

6. Tilakaratne WM, Ekanayaka RP, Herath M, Jayasinghe RD, Sitheeque M, Amarasinghe H. Intralesional corticosteroids as a treatment for restricted mouth opening in oral submucous fibrosis. Oral Surg Oral Med Oral Pathol Oral Radiol. 2016;122:224–31. https://doi.org/10.1016/j.oooo.2015.11.023.

7. Hsieh Y-P, Chen H-M, Lin H-Y, Yang H, Chang JZ-C. Epigallocatechin-3-gallate inhibits transforming-growth-factor-β1-induced collagen synthesis by suppressing early growth response-1 in human buccal mucosal fibroblasts. J Formos Med Assoc. 2017;116:107–13. https://doi.org/10.1016/j.jfma.2016.01.014.

8. Chang JZ-C, Hsieh Y-P, Lin W-H, Chen H-M, Kuo MY-P. Activation of transforming growth factor-β1 by thrombin via integrins αvβ1, αvβ3, and αvβ5 in buccal fibroblasts: Suppression by epigallocatechin-3-gallate. Head Neck. 2017;39:1436–45. https://doi.org/10.1002/hed.24791.

9. Mehta CH, Paliwal S, Muttigi MS, Seetharam RN, Prasad ASB, Nayak Y, et al. Polyphenol-based targeted therapy for oral submucous fibrosis. Inflammopharmacology. 2023;31(5):2349–68. https://doi.org/10.1007/s10787-023-01212-1.

10. Zeng J, Xu H, Cai Y, Xuan Y, Liu J, Gao Y, et al. The effect of ultrasound, oxygen and sunlight on the stability of (−)-epigallocatechin gallate. Molecules. 2018;23(9): 2394. https://doi.org/10.3390/molecules23092394.

11. Mehta CH, Narayan R, Acharya S, Nayak UY. Design and development of surface modified epigallocatechin 3-gallate NanoCubogel for localized delivery to oral submucous fibrosis therapy. J Drug Deliv Sci Technol. 2021;66:102911. https://doi.org/10.1016/j.jddst.2021.102911.

12. Lu H, Zhang S, Wang J, Chen Q. A review on polymer and lipid-based nanocarriers and its application to nano-pharmaceutical and food-based systems. Front Nutr. 2021;8:783831. https://doi.org/10.3389/fnut.2021.783831.

13. Bora A, Sarmah D, Rather MA, Mandal M, Karak N. Nanocomposite of starch, gelatin and itaconic acid-based biodegradable hydrogel and ZnO/cellulose nanofiber: a pH-sensitive sustained drug delivery vehicle. Int J Biol Macromol. 2024;256:128253. https://doi.org/10.1016/j.ijbiomac.2023.128253.

14. Shaikh R, Raj Singh TR, Garland MJ, Woolfson AD, Donnelly RF. Mucoadhesive drug delivery systems. J Pharm Bioallied Sci. 2011;3(1):89–100. https://doi.org/10.4103/0975-7406.76478.

15. Santos TC dos, Rescignano N, Boff L, Reginatto FH, Simões CMO, de Campos AM, et al. Manufacture and characterization of chitosan/PLGA nanoparticles nanocomposite buccal films. Carbohydr Polym. 2017;173:638–44. https://doi.org/10.1016/j.carbpol.2017.06.014.

16. Zhang Y, Zhang J, Chen M, Gong H, Thamphiwatana S, Eckmann L, et al. A bioadhesive nanoparticle–hydrogel hybrid system for localized antimicrobial drug delivery. ACS Appl Mater Interfaces. 2016;8(28):18367–74. https://doi.org/10.1021/acsami.6b04858.

17. Roblegg E, Fröhlich E, Meindl C, Teubl B, Zaversky M, Zimmer A. Evaluation of a physiological in vitro system to study the transport of nanoparticles through the buccal mucosa. Nanotoxicology. 2012;6(4):399–413. https://doi.org/10.3109/17435390.2011.580863.

18. Salama AH, Mahmoud AA, Kamel R. A novel method for preparing surface-modified fluocinolone acetonide loaded PLGA nanoparticles for ocular use: in vitro and in vivo evaluations. AAPS PharmSciTech. 2016;17(5):1159–72. https://doi.org/10.1208/s12249-015-0448-0.

19. Rosita N, Meitasari VA, Rianti MC, Hariyadi DM, Miatmoko A. Enhancing skin penetration of epigallocatechin gallate by modifying partition coefficient using reverse micelle method. Ther Deliv. 2019;10(7):409–17. https://doi.org/10.4155/tde-2019-0015.

20. Avadhani KS, Manikkath J, Tiwari M, Chandrasekhar M, Godavarthi A, Vidya SM, et al. Skin delivery of epigallocatechin-3-gallate (EGCG) and hyaluronic acid loaded nano-transfersomes

for antioxidant and anti-aging effects in UV radiation induced skin damage. Drug Deliv. 2017;24(1):61–74. https://doi.org/10.1080/10717544.2016.1228718.

21. Yurtdaş-Kırımlıoğlu G, Görgülü Ş, Murat &, Berkman S, Ulsel G, Yurtdas Y, et al. Novel approaches to cancer therapy with ibuprofen-loaded Eudragit® RS 100 and/or octadecylamine-modified PLGA nanoparticles by assessment of their effects on apoptosis. Drug Dev Ind Pharm. 2020;46:1133–49. https://doi.org/10.1080/03639045.2020.1776319.

22. Sahu BP, Hazarika H, Bharadwaj R, Loying P, Baishya R, Dash S, et al. Curcumin-docetaxel co-loaded nanosuspension for enhanced anti-breast cancer activity. Expert Opin Drug Deliv. 2016;13(8):1065–74. https://doi.org/10.1080/17425247.2016.1182486.

23. Chen X, Yan J, Yu S, Wang P. Formulation and in vitro release kinetics of mucoadhesive blend gels containing matrine for buccal administration. AAPS PharmSciTech. 2018;19(1):470–80. https://doi.org/10.1208/s12249-017-0853-7.

24. Chiang MH, Lee KT, Chen CH, Chen KK, Wang YH. Photobiomodulation therapy inhibits oral submucous fibrosis in mice. Oral Dis. 2020;26:1474–82. https://doi.org/10.1111/odi.13409.

25. Yesenia K, Hern´hernández-Giottonini H, Rodríguezrodríguez-C´Ordova RJ, Gutí Errez-Valenzuela CA, Peñuñuri O, Peñu P, et al. PLGA nanoparticle preparations by emulsification and nanoprecipitation techniques: effects of formulation parameters. RSC Adv. 2020;10:4218–31. https://doi.org/10.1039/C9RA10857B.

26. Sharma N, Madan P, Lin S. Effect of process and formulation variables on the preparation of parenteral paclitaxel-loaded biodegradable polymeric nanoparticles: a co-surfactant study. Asian J Pharm Sci. 2016;11:404–16. https://doi.org/10.1016/j.ajps.2015.09.004.

27. Nugraheni PS, Soeriyadi AH, Sediawan WB, Ustadi, Budhijanto W. Influence of salt addition and freezing-thawing on particle size and zeta potential of nano-chitosan. IOP Conf Ser Earth Environ Sci. 2019;278:012052. https://doi.org/10.1088/1755-1315/278/1/012052.

28. Zhong W, Zhang T, Dong C, Li J, Dai J, Wang C. Effect of sodium chloride on formation and structure of whey protein isolate/hyaluronic acid complex and its ability to loading curcumin. Colloids Surf A Physicochem Eng Asp. 2022;632:127828. https://doi.org/10.1016/j.colsurfa.2021.127828.

29. Ramesh N, Mandal AKA. Encapsulation of epigallocatechin-3-gallate into albumin nanoparticles improves pharmacokinetic and bioavailability in rat model. 3 Biotech. 2019;9(6):238. https://doi.org/10.1007/s13205-019-1772-y.

30. Deshkar S, Quazi N, Patil A, Poddar S. Effect of Gelucire 44/14 on fluconazole solid lipid nanoparticles: formulation, optimization and in vitro characterization. Drug Deliv Lett. 2016;5(3):173–87. https://doi.org/10.2174/2210303105031601121141.

31. Mohammed WH, Ali WK, Al-Awady MJ. Evaluation of in vitro drug release kinetics and antibacterial activity of vancomycin HCl-loaded nanogel for topical application. J Pharm Sci Res. 2018;10:2747–56. Available from: https://www.jpsr.pharmainfo.in/Documents/Volumes/vol10Issue11/jpsr10111814.pdf. Accessed 11 Dec 2023.

32. Bao Q, Newman B, Wang Y, Choi S, Burgess DJ. In vitro and ex vivo correlation of drug release from ophthalmic ointments. J Control Release. 2018;276:93–101. https://doi.org/10.1016/j.jconrel.2018.03.003.

33. Cevher E, Taha MAM, Orlu M, Araman A. Evaluation of mechanical and mucoadhesive properties of clomiphene citrate gel formulations containing carbomers and their thiolated derivatives. Drug Deliv. 2008;15(1):57–67. https://doi.org/10.1080/10717540701829234.

34. Kamath V, Satelur K, Rajkumar K, Krishnamurthy S. Transforming growth factor beta 1 in oral submucous fibrosis: an immunohistochemical study-understanding the pathogenesis. J Dent Res Rev. 2014;1:75. https://doi.org/10.4103/2348-2915.133942.

35. Rai A, Ahmad T, Parveen S, Parveen S, Faizan MI, Ali S. Expression of transforming growth factor beta in oral submucous fibrosis. J Oral Biol Craniofacial Res. 2020;10(2):166–70. https://doi.org/10.1016/j.jobcr.2020.03.015.

36. Perera J.D.R, Sivakanesan R., Jayasinghe R.D., Bandara B.M.R, Tilakaratne W.M. Role of antioxidants in disease progression and malignant transformation of oral submucous fibrosis (a preliminary study). Sri Lanka Dent J. 2014;44:15–23. Available from: https://www.researchgate.net/publication/293821857_Role_of_Antioxidants_in_Disease_Progression_and_Malignant_Transformation_of_Oral_Submucous_Fibrosis_A_Preliminary_Study. Accessed 21 Dec 2023.

37. Saso L, Reza A, Ng E, Nguyen K, Lin S, Zhang P, et al. A comprehensive analysis of the role of oxidative stress in the pathogenesis and chemoprevention of oral submucous fibrosis. Antioxidants (Basel, Switzerland). 2022;11(5):868. https://doi.org/10.3390/antiox11050868.

38. Kar IB, Sethi AK. A rare ocular complication following treatment of oral submucous fibrosis with steroids. Natl J Maxillofac Surg. 2011;2(1):93–5. https://doi.org/10.4103/0975-5950.85864.

39. Chen H-M, Shih C-C, Yen KL, Wang S-M, Kuo Y-S, Kuo MY-P, et al. Facial Candida albicans cellulitis occurring in a patient with oral submucous fibrosis and unknown diabetes mellitus after local corticosteroid injection treatment. J Oral Pathol Med. 2004;33(4):243–5. https://doi.org/10.1111/j.0904-2512.2004.00058.x.

40. Srikanth G, Komal S, Jyotsna R, Kalyana CP. Unusual complication of intralesional corticosteroid in oral submucous fibrosis patient. Biomed Pharmacol J. 2017;10:1009–13. Available from: http://biomedpharmajournal.org/vol10no2/unusual-complication-of-intralesional-corticosteroid-in-oral-submucous-fibrosis-patient/. Accessed 21 Dec 2023.

41. Pandya D, Nagrajappa AK, Ravi KS. Assessment and correlation of urea and creatinine levels in saliva and serum of patients with chronic kidney disease, diabetes and hypertension- a research study. J Clin Diagnostic Res. 2016;10(10):ZC58–62. https://doi.org/10.7860/JCDR/2016/20294.8651.

42. Kleynhans J, Elgar D, Ebenhan T, Zeevaart JR, Kotzé A, Grobler A. A toxicity profile of the Pheroid® technology in rodents. Toxicol reports. 2019;6:940–50. https://doi.org/10.1016/j.toxrep.2019.08.012.

43. Mainardes RM, Evangelista RC. PLGA nanoparticles containing praziquantel: effect of formulation variables on size distribution. Int J Pharm. 2005;290(1-2):137–44. https://doi.org/10.1016/j.ijpharm.2004.11.027.

44. Pool H, Quintanar D, Figueroa JDD, Marinho Mano C, Bechara JEH, Godínez LA, et al. Antioxidant effects of quercetin and catechin encapsulated into PLGA nanoparticles. J Nanomater. 2012;2012. https://doi.org/10.1155/2012/145380.

45. Badri W, Miladi K, Robin S, Viennet C, Nazari QA, Agusti G, et al. Polycaprolactone based nanoparticles loaded with indomethacin for anti-inflammatory therapy: from preparation to ex vivo study. Pharm Res. 2017;34(9):1773–83. https://doi.org/10.1007/s11095-017-2166-7.

46. Narayanan K, Subrahmanyam VM, Venkata Rao J. A fractional factorial design to study the effect of process variables on the preparation of hyaluronidase loaded PLGA nanoparticles. Enzyme Res. 2014:2014; 162962. https://doi.org/10.1155/2014/1629622.

47. Keum CG, Noh YW, Baek JS, Lim JH, Hwang CJ, Na YG, et al. Practical preparation procedures for docetaxel-loaded nanoparticles using polylactic acid-co-glycolic acid. Int J Nanomedicine. 2011;6:2225–34. https://doi.org/10.2147/IJN.S24547.

48. Feczkó T, Tóth J, Dósa G, Gyenis J. Influence of process conditions on the mean size of PLGA nanoparticles. Chem Eng Process Process Intensif. 2011;50:846–53. https://doi.org/10.1016/j.cep.2011.05.006.

49. Srivastava AK, Bhatnagar P, Singh M, Mishra S, Kumar P, Shukla Y, et al. Synthesis of PLGA nanoparticles of tea polyphenols and their strong in vivo protective effect against chemically induced DNA damage. Int J Nanomedicine. 2013;8:1451–62. https://doi.org/10.2147/IJN.S26364.

50. Dahiya S, Rani R, Dhingra D, Kumar S, Dilbaghi N. Conjugation of epigallocatechin gallate and piperine into a zein nanocarrier: Implication on antioxidant and anticancer potential. Adv Nat Sci Nanosci Nanotechnol. 2018;9:035011. https://doi.org/10.1088/2043-6254/aad5c1.

51. Hua S. Advances in nanoparticulate drug delivery approaches for sublingual and buccal administration. Front Pharmacol. 2019;10:1328. https://doi.org/10.3389/fphar.2019.01328.

52. Swarnakar NK, Jain V, Dubey V, Mishra D, Jain NK. Enhanced oromucosal delivery of progesterone via hexosomes. Pharm Res. 2007;24:2223–30. https://doi.org/10.1007/s11095-007-9409-y.

53. Butreddy A, Narala A, Dudhipala N. Formulation and characterization of liquid crystalline hydrogel of agomelatin: in vitro and ex vivo evaluation. J Appl Pharm Sci. 2015;5:110–4. https://doi.org/10.7324/JAPS.2015.50920.

54. Holpuch AS, Hummel GJ, Tong M, Seghi GA, Pei P, Ma P, et al. Nanoparticles for local drug delivery to the oral mucosa: proof of principle studies. Pharm Res. 2010;27(7):1224–36. https://doi.org/10.1007/s11095-010-0121-y.

55. Sadaksharam J. Significance of serum nitric oxide and superoxide dismutase in oral submucous fibrosis and squamous cell carcinoma: a comparative study. Contemp Clin Dent. 2018;9(2):283–8. https://doi.org/10.4103/ccd.ccd_11_18.

56. Banerjee S, Mukherjee S, Mitra S, Singhal P. Comparative evaluation of mitochondrial antioxidants in oral potentially malignant disorders. Kurume Med J. 2020;66(1):15–27. https://doi.org/10.2739/kurumemedj.ms661009.